The oldest rocks of Greece: first evidence for a Precambrian terrane within the Pelagonian Zone

B. ANDERS*‡§, T. REISCHMANN*‡, D. KOSTOPOULOS† & U. POLLER‡

*Institut für Geowissenschaften, Becherweg 21, Johannes Gutenberg-Universität Mainz, 55099 Mainz, Germany
†Department of Mineralogy and Petrology, National and Kapodistrian University of Athens,
Panepistimioupoli Zographou, Athens 15784, Greece
‡Max-Planck-Institut für Chemie, Abt. Geochemie, Postfach 3060, 55020 Mainz, Germany

Abstract – The Pelagonian Zone in Greece represents the westernmost belt of the Hellenide hinterland (Internal Hellenides). Previous geochronological studies of basement rocks from the Pelagonian Zone have systematically yielded Permo-Carboniferous ages. In this study we demonstrate, for the first time, the existence of a Precambrian crustal unit within the crystalline basement of the Pelagonian Zone. The U–Pb single-zircon and SHRIMP ages of these orthogneisses vary from 699 ± 7 Ma to 713 ± 18 Ma, which identify them as the oldest rocks in Greece. These Late Proterozoic rocks, which today occupy an area of *c*. 20×100 km, are significantly different from the neighbouring rocks of the Pelagonian Zone. They are therefore interpreted as delineating a terrane, named here the Florina Terrane. During the Permo-Carboniferous, Florina was incorporated into an active continental margin, where it formed part of the basement for the Pelagonian magmatic arc. The activity of this arc was dated in this study by single-zircon Pb/Pb ages as having taken place at 292 ± 5 Ma and 298 ± 7 Ma. During the Alpine orogeny, Florina, together with the Pelagonian Zone, eventually became a constituent of the Hellenides. Geochemically, the Florina orthogneisses represent granites formed at an active continental margin. Because of the Late Proterozoic ages, this Late Proterozoic active continental margin can be correlated to a Pan-African or Cadomian arc. As the gneisses contain inherited zircons of Late to Middle Proterozoic age, the original location of Florina was probably at the northwestern margin of Gondwana. Similar to other Gondwana-derived terranes, such as East Avalonia, Florina approached the southern margin of Eurasia during Palaeozoic times, where it became part of an active continental margin above the subducting Palaeotethys. These interpretations further indicate that terrane accretion was already playing an important role in the early pre-alpine evolution of the Hellenides.

Keywords: zircon geochronology, Nd isotopes, Neoproterozoic basement, Florina Terrane, Pelagonian Zone, Greece.

1. Introduction and geological background

In the eastern Mediterranean, the Hellenides constitute an integral part of the Alpine–Himalayan orogenic belt. The Hellenides are traditionally divided into the Internal Hellenides (the Greek hinterland) with abundant occurrences of gneissic and granitic basement rocks, and the External Hellenides (the Greek foreland), built up by Mesozoic and Cenozoic cover rocks (e.g. Aubouin *et al.* 1963; see also Jacobshagen, 1986). The Internal Hellenides are further subdivided into several tectonostratigraphic zones, which are, from NE to SW: the Rhodope Massif, the Serbo-Macedonian Massif, the Vardar Zone, the Pelagonian Zone and the Attico-Cycladic Massif (e.g. Aubouin *et al.* 1963; see also Jacobshagen, 1986).

The Neoproterozoic to Tertiary evolution of the Mediterranean realm, especially the eastern Mediter-

ranean, includes the opening and closure of multiple ocean basins (e.g. Şengör & Yilmaz, 1981; Stampfli & Borel, 2002; von Raumer, Stampfli & Bussy, 2003). Subduction-related magmatism is widespread, and possible tectonic settings include intra-oceanic volcanic-arc magmatism as well as magmatism in an active continental-margin setting, either along the northern margin of Gondwana or the southern margin of Baltica/Europe. Generally, geochemistry and dating of magmatic rocks can discriminate between different tectonic settings, lead to the identification of distinct terranes and help to constrain their evolutionary history (Pearce, Harris & Tindle, 1984; Nance & Murphy, 1994; Friedl *et al.* 2000). Here, we have used geochemical and geochronological tools to decipher a possible multiphase evolution of the basement rocks from the Pelagonian Zone.

The Pelagonian Zone forms an elongated NNW–SSE-trending zone (Fig. 1a). Towards the north it continues into the Former Yugoslav Republic of

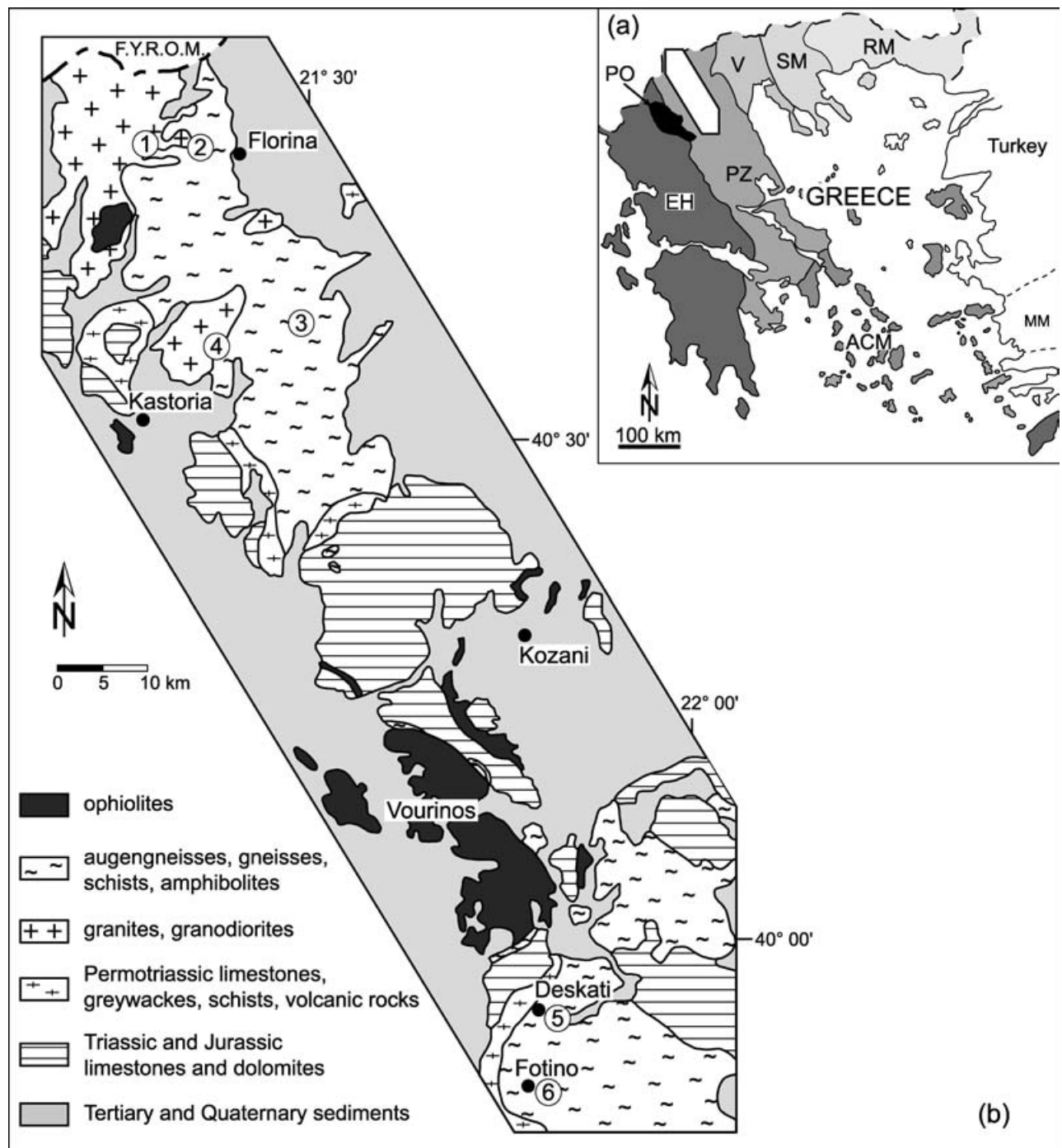§ Author for correspondence: banders@mail.uni-mainz.de

Figure 1. (a) Map showing the tectonostratigraphic zones of the Hellenides. RM – Rhodope Massif; SM – Serbo-Macedonian Massif; V – Vardar Zone; PZ – Pelagonian Zone; ACM – Attico-Cycladic Massif; EH – External Hellenides; PO – Pindos ophiolite; MM – Menderes Massif. (b) Geological map of the study area, simplified after the geological map of Greece 1:500 000 (IGME, 1983). Sample localities: 1 – Varnous granodiorite V1; 2 – Varnous orthogneiss V9; 3 – Florina orthogneisses Pl58 and Pl59; 4 – Kastoria granite Pl61; 5 – Deskati orthogneiss Pl70; 6 – Fotino granite Pl64-Pl66. F.Y.R.O.M. – Former Yugoslav Republic of Macedonia.

Macedonia (F.Y.R.O.M.), while in the south it is bordered by the Attico-Cycladic Massif (Fig. 1a). The Greek part of the Pelagonian Zone consists of granitic and gneissic basement rocks, Mesozoic metasedimentary rocks and Tertiary to recent sediments (e.g. Jacobshagen, 1986 and references therein; Pe-Piper & Piper, 2002 and references therein). Outcrops of

basement rocks are discontinuous, although all geochronological results reported so far show that their ages are rather uniform, ranging from 280 to 320 Ma (e.g. Yarwood & Aftalion, 1976; Mountrakis, 1984; Koroneos et al. 1993; Katerinopoulos et al. 1998; Vavassis et al. 2000; Reischmann et al. 2001; Anders et al. 2003). Geochemical fingerprinting favours a

subduction-zone environment as the origin for the basement rocks of the Pelagonian Zone, most probably in a volcanic-arc or active continental-margin setting (e.g. Pe-Piper, Doutsos & Mijara, 1993; Pe-Piper, Doutsos & Mporonkay, 1993; Katerinopoulos *et al.* 1998; Vavassis *et al.* 2000, Reischmann *et al.* 2001; Anders *et al.* 2003). This leads to the interpretation of the Pelagonian Zone as a large Permo-Carboniferous magmatic arc (e.g. Reischmann *et al.* 2001; Anders *et al.* 2003). However, an active continental-margin setting would require the existence of older, pre-Carboniferous continental basement. To date, only structural and stratigraphical observations indicated the existence of Lower Palaeozoic or older basement in the Pelagonian Zone as was, for example, inferred from intrusive contacts of an Upper Carboniferous granite in gneissic country rocks by Mountrakis (1984). A. Kilias (unpub. Ph.D. thesis, Univ. Thessaloniki, 1980) and Marakis (1969) obtained Lower Palaeozoic K–Ar ages for rocks from the northern Pelagonian Zone in Greece and its northward continuation into F.Y.R.O.M., but attributed these old ages to excess Ar. Most (2001, 2003) undertook a geochronological study of rocks from the northwest Pelagonian Zone in southern F.Y.R.O.M. and measured a Silurian K–Ar age (447 ± 17 Ma) for white mica extracted from a granite. However, zircons from the same sample dated by the U–Pb method yielded a Permian age (246 ± 7 Ma). Most (2003) explained this discrepancy by invoking excess Ar due to metasomatic alteration. It is therefore clear from the above that the question of the existence of Lower Palaeozoic or older magmatic rocks in the Pelagonian Zone has not yet been answered. In the Attico-Cycladic Massif, which can be regarded as the southern extension of the Pelagonian Zone, basement rocks show the same range of Permo-Carboniferous ages, clustering around *c*. 300 Ma (Engel & Reischmann, 1998; Reischmann, 1998). No evidence for older magmatic rocks exists for the Cycladic islands.

In our study we focused on the geochronology and geochemistry of basement rocks from the northwestern part of the Pelagonian Zone in Greece. The aim was to improve geochronological resolution and follow up the question of Early to Mid-Palaeozoic ages of the westernmost Internal Hellenide Zones, as well as to characterize geochemically the basement rocks with regard to their possible tectonic setting. Special emphasis was put on single-zircon dating, because zircons (a) are abundant accessory minerals in felsic rocks, (b) strongly incorporate Th and U but only minor amounts of Pb, thus making them suitable for U–Pb dating, (c) have a high closure temperature for the U–Pb system (e.g. Lee, Williams & Ellis, 1997; Cherniak & Watson, 2000), allowing dating of the intrusion event, and (d) are resistant to resetting of the U–Pb isotopic system during later metamorphic events or alteration (e.g. Parrish, 2001; Corfu *et al.* 2003). Orthogneisses

and granitic basement rocks were sampled from the Florina, Kastoria and Fotino localities (see Fig. 1b) and are discussed in detail below.

2. Analytical methods

Zircons were dated using the single-zircon Pb/Pb evaporation technique (Kober, 1986, 1987), the single-zircon conventional U–Pb method and by sensitive high-resolution ion microprobe (SHRIMP). Dating with the conventional U–Pb method was based on the low-contamination dissolution method of Krogh (1973), two variants of which were used: (a) the vapour-digestion method (Wendt & Todt, 1991) and (b) the chemical separation of Pb and U by HBr chemistry following dissolution. The measurements were performed with a Finnigan MAT 261 thermal ionization mass-spectrometer (TIMS) at the Max-Planck-Institut für Chemie, Mainz, Germany, using an ion multiplier. The measured ratios were corrected for fractionation (3‰ per ΔAMU), blank and common Pb (using the values given by Stacey & Kramers, 1975). The fractionation factor was determined by measuring NBS 981 under the same conditions as the samples. Total procedure blanks for Pb were < 10 pg for vapour digestion and < 40 pg for chemical separation. Ages were calculated using Isoplot (Ludwig, 2003).

One sample was dated by SHRIMP at the Centre of Isotopic Research, St Petersburg, Russia. The TEMORA reference zircon (age 416.75 Ma: Black *et al.* 2003) was used for calibration of the Pb–U ratios. Data reduction and age calculations were based on SQUID (Ludwig, 2001).

Concordia diagrams were drawn using Isoplot (Ludwig, 2003). All ages are given either at the 2σ or 95 % confidence level. Calculation of the weighted average was based on Ludwig (2003).

Whole-rock Sr- and Nd-isotope compositions were measured with a Finnigan MAT 261 TIMS in multi-collector mode at the Max-Planck-Institut für Chemie, Mainz, Germany. Sample preparation was based on standard procedures as described in White & Patchett (1984). Mass fractionation of Nd and Sr was corrected to ^{146}Nd/^{144}Nd $= 0.7219$ and ^{86}Sr/^{88}Sr $= 0.1194$, respectively. During the course of this study, repeated analyses of the La Jolla standard resulted in a measured ^{143}Nd/^{144}Nd value of 0.511823 ± 20 (95 % conf., n $= 7$). To allow comparison between samples measured on different days, all ^{143}Nd/^{144}Nd values were adjusted to this ratio. For the NBS SRM 987 an ^{87}Sr/^{86}Sr value of 0.710234 ± 12 (2σ, n $= 16$) was obtained.

3. Sample description and geochronological results

Sample description and geochronological results are arranged in this paper from north to south (Fig. 1b). Geochronological data are presented in Tables 1–3.

Table 1. Data of single-zircon Pb/Pb evaporation analyses

Sample-grain	Number of ratios	$^{206}Pb/^{204}Pb^1$	$^{207}Pb*/^{206}Pb*^2$	$\pm 2\sigma$	Age (Ma)	$\pm 2\sigma$
V1-A	131	9027	0.052156	0.000089	292	4
V1-B	124	10994	0.052246	0.000038	296	2
V1-C	87	8995	0.052130	0.000083	291	4
V1-D	170	7657	0.052034	0.000080	287	4
V1-E	113	5782	0.052384	0.000051	302	2
V1-F	131	8140	0.052466	0.000056	306	2
V1-G	59	8338	0.051115	0.000391	246	18
V9-A	134	8836	0.061591	0.000105	660	4
V9-B	109	27394	0.069183	0.000245	904	7
V9-C	76	12395	0.108649	0.000798	1777	13
V9-D	135	8949	0.061133	0.000083	644	3
V9-E	91	13407	0.062223	0.000141	682	5
V9-F	138	11636	0.062218	0.000092	682	3
V9-G	126	15070	0.063693	0.000103	731	3
V9-H	138	14144	0.062412	0.000079	688	3
Pl61-A	151	6599	0.052081	0.000106	289	5
Pl61-B	149	3198	0.052082	0.000084	289	4
Pl61-C	172	5989	0.052047	0.000060	287	3
Pl61-D	91	14153	0.052303	0.000111	299	5
Pl61-E	113	13423	0.052256	0.000076	297	3
Pl61-F	154	1896	0.052333	0.000157	300	7

[1] Measured ratio; [2] Radiogenic Pb, ratios corrected for common Pb.

The northernmost samples are V1 and V9, collected west of Florina town (Fig. 1b). Sample V1 is a rather coarse-grained igneous rock from the Varnous pluton. It consists mainly of quartz, K-feldspar, plagioclase and biotite, together with titanite and fine-grained epidote/zoisite. Remnants of amphibole also occur. Secondary alteration is indicated by the partial sericitization of K-feldspar and partial conversion of titanite to leucoxene. The rock was dated by the single-zircon Pb/Pb evaporation method (Kober, 1986, 1987). The analyses of six zircon grains resulted in $^{207}Pb/^{206}Pb$ ages of between 287 ± 4 Ma and 306 ± 2 Ma. There are two possible explanations for the lack of overlap of the ages within error. Firstly, the relatively small errors of the ages are probably underestimated because they are largely dependent on measurement statistics, and a large number of $^{207}Pb/^{206}Pb$ ratios measured for each grain will produce small errors. The average age would then be meaningful and, in the case of this sample, date the intrusion event. A second possible explanation for the spread in ages is influence by a younger thermal event resulting in Pb loss and younger $^{207}Pb/^{206}Pb$ ages. In this case the younger ages would reflect stronger Pb loss and only the oldest ages would approximate the intrusion age (assuming that no inherited Pb component exists). In the case of sample V1, evidence for Pb loss is demonstrated in one grain with a significantly younger $^{207}Pb/^{206}Pb$ age of 246 ± 18 Ma. Cathodoluminescence (CL) images of zircons show clear, fine-scale oscillatory zoning that is interpreted to reflect magmatic growth and changing chemical conditions along zircon grain boundaries (e.g. oversaturation, diffusion rate) in the magma chamber (Vavra, 1990; Mattinson *et al.* 1996). Several zircon grains show homogeneous, light-grey, low-U domains that irregularly cross-cut the oscillatory zoning in CL
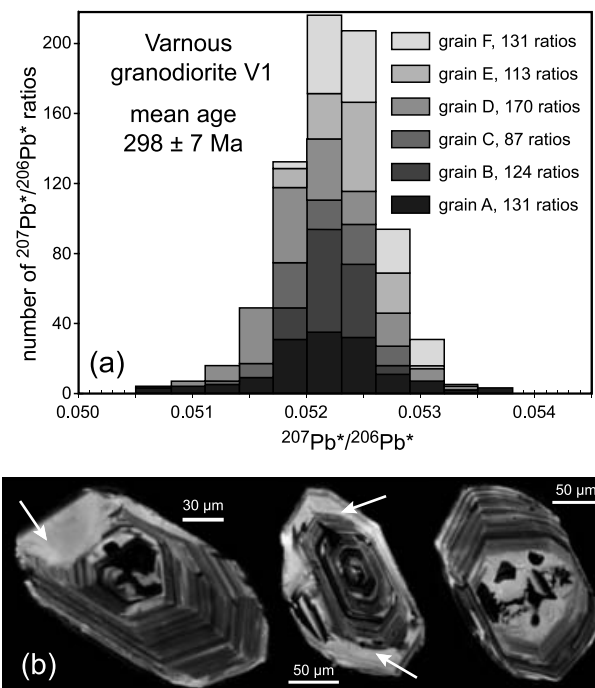
Figure 2. (a) Histogram presenting single-zircon Pb/Pb evaporation analyses for Varnous granodiorite V1. (b) CL images of zircons from granodiorite V1, showing fine-scale magmatic zoning and recrystallized and resorbed parts of the zircons. Arrows indicate regions that cross-cut the oscillatory zoning.

images (Fig. 2b). These zones are possibly due to recrystallization, either during a late magmatic stage or metamorphism, where Pb-loss is more likely (Connelly, 2000). The irregular and sometimes convolute zones in the cores of several zircons are also interpreted as recrystallized parts. They might also indicate zircon domains affected by Pb loss. No indications for inherited cores were seen in CL images. The age group,

Table 2. Results of conventional U–Pb single-zircon geochronology

Sample	Grain	$^{206}Pb/^{204}Pb^1$	2σ	$^{206}Pb/^{207}Pb^1$	2σ	$^{207}Pb/^{235}U^2$	2σ	$^{206}Pb/^{238}U^2$	2σ	R	$^{206}Pb/^{207}Pb^2$	2σ	U_{tot}/Pb_{rad}	$^{206}Pb/^{238}U^3$ Age (Ma)	2σ	$^{207}Pb/^{235}U^3$ Age (Ma)	2σ	$^{206}Pb/^{207}Pb^3$ Age (Ma)	2σ
V9	a	3961	298	0.06630	0.00011	0.8758	0.0115	0.10123	0.00069	0.74	0.06275	0.00039	8.6	622	4	639	6	700	13
V9	b	2802	87	0.06753	0.00018	0.8675	0.0105	0.10079	0.00065	0.73	0.06243	0.00037	8.4	619	4	634	6	689	13
V9	c	2077	29	0.06920	0.00006	0.8620	0.0073	0.10030	0.00059	0.90	0.06233	0.00017	8.6	616	3	631	4	686	6
V9	d	2307	43	0.06822	0.00018	0.8475	0.0157	0.09906	0.00133	0.93	0.06205	0.00033	8.4	609	8	623	9	676	11
V9	e	1772	11	0.07039	0.00005	0.8359	0.0060	0.09732	0.00053	0.93	0.06230	0.00013	8.8	599	3	617	3	684	4
V9	f	351	1	0.10221	0.00010	0.6676	0.0058	0.07938	0.00034	0.53	0.06100	0.00040	11.1	492	2	519	4	639	14
V9	g	1257	44	0.07566	0.00016	1.0226	0.0140	0.11520	0.00054	0.44	0.06438	0.00056	7.5	703	3	715	7	754	19
Pl58	h	1130	17	0.08382	0.00019	1.4398	0.0172	0.14632	0.00076	0.65	0.07137	0.00041	6.2	880	4	906	7	968	12
Pl58	i	2172	25	0.08304	0.00013	1.4991	0.0109	0.14194	0.00063	0.84	0.07660	0.00022	6.4	856	4	930	4	1111	6
Pl58	j	1010	13	0.08417	0.00004	1.3346	0.0155	0.13797	0.00108	0.92	0.07016	0.00023	6.6	833	6	861	7	933	7
Pl58	k	835	9	0.09389	0.00008	1.4542	0.0148	0.13713	0.00089	0.81	0.07691	0.00035	6.4	828	5	912	6	1119	9
Pl58	l	424	8	0.09732	0.00011	1.0910	0.0230	0.12386	0.00084	0.52	0.06389	0.00066	7.2	753	5	749	11	738	22
Pl58	m	503	7	0.09468	0.00025	1.0916	0.0276	0.11916	0.00136	0.64	0.06644	0.00086	7.5	726	8	749	14	820	27
Pl58	n	371	12	0.10860	0.00068	1.1215	0.0493	0.11575	0.00139	0.28	0.07027	0.00255	7.7	706	8	764	24	936	76
Pl58	o	300	6	0.11382	0.00030	1.0422	0.0320	0.11429	0.00095	0.26	0.06614	0.00170	7.9	698	5	725	16	811	55
Pl58	p	848	12	0.08034	0.00014	1.0026	0.0132	0.11423	0.00068	0.75	0.06365	0.00032	7.9	697	4	705	7	730	11
Pl58	q	426	3	0.09776	0.00013	0.9931	0.0118	0.11240	0.00056	0.48	0.06408	0.00054	8.1	687	3	700	6	744	18
Pl58	r	1690	15	0.07249	0.00006	0.8987	0.0062	0.10174	0.00046	0.89	0.06406	0.00014	9.0	625	3	651	3	744	5
Pl58	s	849	9	0.07892	0.00007	0.8530	0.0084	0.09972	0.00048	0.70	0.06204	0.00030	8.7	613	3	626	5	675	10
Pl58	t	633	18	0.08544	0.00035	0.8016	0.0347	0.09287	0.00248	0.63	0.06260	0.00197	9.4	572	15	598	20	695	69
Pl59	u	456	1	0.11652	0.00011	1.9157	0.0123	0.16172	0.00062	0.75	0.08592	0.00028	5.2	966	3	1087	4	1336	6
Pl59	v	451	5	0.10723	0.00014	1.6751	0.0301	0.16007	0.00161	0.66	0.07590	0.00084	5.6	957	9	999	11	1092	22
Pl59	w	264	4	0.12317	0.00037	1.1474	0.0356	0.12058	0.00138	0.42	0.06901	0.00158	7.4	734	8	776	17	899	48
Pl59	x	1766	74	0.08150	0.00006	1.0122	0.0108	0.09995	0.00052	0.64	0.07345	0.00043	8.9	614	3	710	5	1027	12
Pl59	y	409	3	0.10257	0.00006	0.8276	0.0107	0.08898	0.00075	0.80	0.06746	0.00042	10.3	550	4	612	6	852	13
Pl70	z	281	3	0.11370	0.00021	0.9207	0.0257	0.10665	0.00117	0.41	0.06261	0.00140	7.5	653	7	663	14	695	48
Pl70	aa	2881	30	0.06766	0.00011	0.9001	0.0064	0.10412	0.00046	0.85	0.06270	0.00017	7.9	638	3	652	3	698	6
Pl70	bb	703	10	0.08363	0.00011	0.9045	0.0130	0.10378	0.00074	0.60	0.06321	0.00057	8.2	637	4	654	7	715	19
Pl70	cc	912	4	0.07849	0.00004	0.8792	0.0082	0.10173	0.00076	0.95	0.06269	0.00016	7.8	625	4	641	4	698	5
Pl70	dd	1768	41	0.08896	0.00014	1.6716	0.0169	0.14956	0.00086	0.77	0.08106	0.00037	5.8	899	5	998	6	1223	9
Pl70	ee	1939	15	0.08251	0.00008	1.3082	0.0079	0.12602	0.00050	0.90	0.07529	0.00014	6.4	765	3	849	3	1076	4
Pl64	ff	619	6	0.08544	0.00026	0.8953	0.0117	0.10454	0.00048	0.38	0.06211	0.00064	7.9	641	3	649	6	678	22
Pl64	gg	195	2	0.13570	0.00015	0.8569	0.0192	0.10132	0.00068	0.27	0.06134	0.00128	8.0	622	4	628	11	651	45
Pl64	hh	167	1	0.14822	0.00033	0.7990	0.0314	0.09392	0.00154	0.26	0.06170	0.00341	8.8	579	9	596	18	664	123
Pl64	ii	704	5	0.07975	0.00008	0.5103	0.0054	0.06256	0.00041	0.75	0.05916	0.00033	13.9	391	2	419	4	573	12
Pl64	jj	385	2	0.09586	0.00026	0.4787	0.0062	0.05965	0.00022	0.28	0.05821	0.00067	14.5	374	1	397	4	538	25
Pl66	kk	542	3	0.08895	0.00009	0.8790	0.0106	0.10226	0.00079	0.73	0.06234	0.00043	8.4	628	5	640	6	686	15
Pl66	ll	736	9	0.08168	0.00020	0.8417	0.0108	0.09827	0.00055	0.54	0.06212	0.00051	8.4	604	3	620	6	678	18
Pl66	mm	771	1	0.07997	0.00003	0.7043	0.0047	0.08335	0.00046	0.95	0.06129	0.00011	10.5	516	3	541	3	649	4
Pl66	nn	828	7	0.07804	0.00013	0.6428	0.0079	0.07686	0.00034	0.79	0.06065	0.00034	11.4	477	3	504	5	627	12
Pl66	oo	302	1	0.13165	0.00011	1.7797	0.0142	0.15166	0.00064	0.54	0.08511	0.00054	5.7	910	4	1038	5	1318	12
Pl66	pp	1035	10	0.08560	0.00010	1.2963	0.0131	0.13068	0.00084	0.86	0.07195	0.00027	6.7	792	5	844	6	984	8

^{1} Measured ratios; ^{2} Ratios corrected for spike, fractionation and common Pb; ^{3} Apparent ages.

Table 3. Results of U–Pb SHRIMP analyses

| Sample | Grain. spot | U (ppm) | Th (ppm) | Th/U | $^{206}Pb_{rad}$ (ppm) | $^{204}Pb/^{206}Pb$ | $^{206}Pb_c$ (%) | Radiogenic ratios, SQUID corrected[1] | | | | R | Age (Ma) $^{206}Pb/^{238}U$ | | Age (Ma) $^{207}Pb/^{206}Pb$ | |
								$^{207}Pb/^{235}U$	±* (%)	$^{206}Pb/^{238}U$	±* (%)			±*		±*
Pl58	1.1	286	43	0.15	28.2	—[2]	—	1.029	1.4	0.1147	0.67	0.464	700	5	777	27
Pl58	2.1	369	76	0.20	36.5	0.00012	0.21	0.994	1.7	0.1150	0.61	0.356	702	4	698	34
Pl58	3.1	242	54	0.22	24.3	0.00015	0.27	1.022	2.3	0.1167	0.71	0.308	711	5	726	47
Pl58	3.2	186	264	1.42	42.1	0.00011	0.18	3.390	1.2	0.2620	0.68	0.551	1500	9	1505	20
Pl58	4.1	178	47	0.26	16.3	0.00030	0.53	0.894	3.5	0.1063	0.83	0.233	651	5	637	74
Pl58	5.1	223	52	0.23	22.5	0.00005	0.10	1.029	2.1	0.1175	0.72	0.345	716	5	725	42
Pl58	1.2	202	48	0.24	20.4	0.00015	0.26	1.025	2.7	0.1178	0.75	0.275	718	5	712	56
Pl58	6.1	682	124	0.18	71.6	0.00002	0.04	1.062	1.0	0.1220	0.50	0.506	741	4	711	18
Pl58	7.1	792	72	0.09	75.9	0.00006	0.10	0.949	1.1	0.1114	0.49	0.442	681	3	666	21
Pl58	8.1	249	66	0.26	24.7	0.00006	0.11	1.018	2.2	0.1151	0.70	0.321	702	5	746	44
Pl58	9.1	167	71	0.43	16.8	0.00028	0.48	0.995	3.0	0.1170	0.84	0.282	713	6	662	61
Pl58	9.2	338	49	0.15	34.1	0.00016	0.28	1.028	1.8	0.1172	0.64	0.354	714	4	729	36
Pl58	10.1	465	44	0.10	46.4	0.00007	0.12	1.000	1.5	0.1161	0.57	0.374	708	4	689	30

* Errors are 1σ; $^{206}Pb_{rad}$ and $^{206}Pb_c$ indicate the radiogenic and common Pb portions, respectively.
[1] Errors in standard calibration (Temora reference zircon) was 0.25 % (not included in the above errors).
[2] For this spot counts on ^{204}Pb were below background level, a $^{204}Pb/^{206}Pb$ ratio of 0.000001 was then assumed to perform the common Pb correction.

which may still be regarded as fairly homogeneous, implies that possible Pb loss did not severely affect the $^{207}Pb/^{206}Pb$ ratios in six out of seven grains, and we suggest that the weighted average minimum age of 298 ± 7 Ma sufficiently approximates the intrusion event. The relatively large error of ± 7 Ma might then account for this uncertainty. The zircon age of this study is in good agreement with a Rb–Sr errorchron age of 297 ± 25 Ma (whole-rock and biotite) obtained by Koroneos *et al.* (1993) on igneous rocks from the Varnous pluton.

Sample V9 was taken from the country rock into which the Varnous pluton apparently intruded. It is a medium-grained, foliated orthogneiss with small feldspar 'augen'. The main minerals are quartz, K-feldspar, white mica, biotite, plagioclase and minor epidote. The rims of the K-feldspars show recrystallization, which is an indication of metamorphism at upper greenschist to lower amphibolite facies conditions. For this sample, the Pb/Pb evaporation method resulted in a wide range of individual zircon ages with a broad peak at about 680 ± 31 Ma (Fig. 3a) and distinctly older $^{207}Pb/^{206}Pb$ ages for two zircon grains at 904 ± 7 Ma and 1777 ± 13 Ma respectively (grains V9-B and V9-C, Table 1). To obtain better accuracy and precision on the age, the conventional single-zircon U–Pb method was also applied. In a concordia diagram, the resulting upper intercept age of 713 ± 18 Ma (MSWD = 0.86) is interpreted as the emplacement age (Fig. 3b). The lower intercept age of 187 ± 59 Ma is attributed to Pb loss. One grain (grain g, Fig. 3b) has evidently inherited some older component, shown in a $^{207}Pb/^{206}Pb$ age of 754 ± 19 Ma. The existence of inherited components, as indicated by older $^{207}Pb/^{206}Pb$ ages obtained from both the Pb/Pb and the U–Pb method on sample V9, can be seen in CL images of zircons that show rounded cores (Fig. 3c).
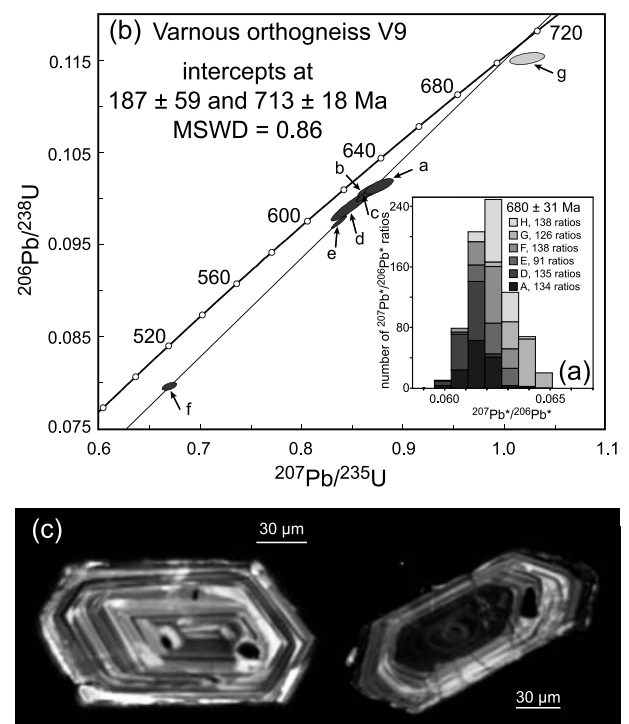

Figure 3. (a) Histogram showing the results of single-zircon Pb/Pb evaporation dating for Varnous orthogneiss V9; two older grains are not shown (see Table 1). (b) Concordia diagram for Varnous orthogneiss V9 (single-zircon conventional U–Pb measurements). Error ellipses are 2σ. The light-coloured ellipse (grain g) in the concordia diagram displays an inherited grain that was not included in the age calculation. (c) CL images showing clear single-phase magmatic zoning (left grain); rounded parts can also be seen (right grain).

The area southeast of Florina is characterized by exposures of amphibolites, paragneisses and orthogneisses. A rather coarse-grained orthogneiss was sampled approximately 20 km southeast of Florina. Samples Pl58 and Pl59 were taken from the same rock
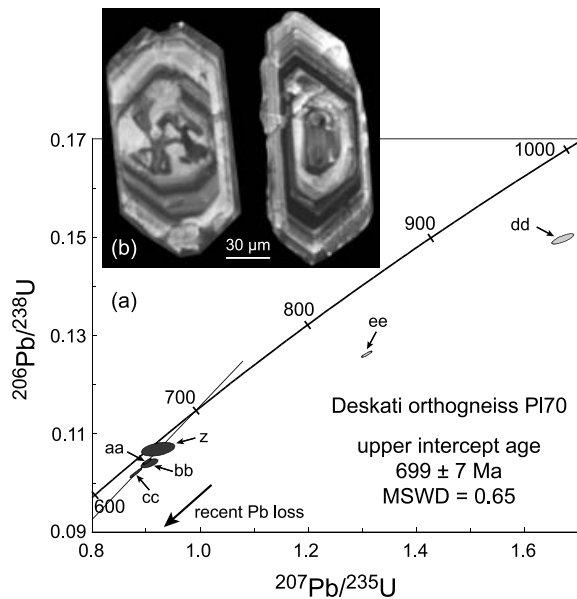
Figure 4. (a) Concordia diagram for Florina orthogneisses Pl58 and Pl59 (single-zircon conventional U–Pb measurements). Note that many single-grain analyses cluster around 700 Ma. (b) SHRIMP results for sample Pl58. Error ellipses are at the 2σ level. The CL image shows the complex structure of a zircon with Middle Proterozoic core and Neoproterozoic rim.

Figure 5. (a) Histogram displaying the results of single-zircon Pb/Pb evaporation analyses for the Kastoria granite Pl61. (b) CL images showing the predominance of fine-scale magmatic growth zoning and the presence of resorbed and recrystallized areas.

unit *c.* 100–200 m apart. The gneisses consist mainly of quartz, K-feldspar, plagioclase, white mica, biotite and minor epidote. Single-zircon conventional U–Pb dating of both samples resulted in a large scatter of zircon grains in a concordia diagram (Fig. 4a) that makes the assignment of an intrusion age impossible. The scatter can be explained by inherited component(s) and one or more thermal/metamorphic events resulting in Pb loss. Inherited cores were not visible under the binocular microscope but are abundant in the CL images. Zircons of orthogneiss Pl58 were therefore dated with SHRIMP (Fig. 4b). Assuming that the rims reflect the magmatic intrusion event of the rock, SHRIMP measurements focused on analysing the rims of the zircons. Eight analyses resulted in a concordant age of 710 ± 5 Ma (MSWD = 0.98) that is interpreted as the intrusion age of the rock. One discordant spot (1.1) was not included in the age calculation. The analysis of one core (3.2)

gave an age of *c.* 1500 Ma, which was taken to indicate the age of an inherited component. Two younger rim ages of *c.* 650 and 680 Ma (spots 4.1 and 7.1, Fig. 4b) are interpreted to reflect Pb loss.

The Kastoria granite is a large, deformed granitic body that is exposed east of the town of Kastoria. The granite was sampled from an outcrop about 10 kilometres west of the localities of Florina orthogneisses Pl58 and Pl59. Deformed granite Pl61 consists mainly of K-feldspar, quartz, saussuritized plagioclase, amphibole, sericite, apatite, titanite, remnants of biotite and epidote. It is a greenish granite with large angular K-feldspar crystals. The granite was dated by the single-zircon Pb/Pb evaporation method. The analyses of six zircons resulted in an age of 292 ± 5 Ma, which is interpreted as the intrusion age (Fig. 5a). This interpretation is supported by CL images of zircons that show single-stage magmatic-growth oscillatory zoning (Fig. 5b). In some CL images, diffuse areas of resorption can be seen. Resorption can take place in a magma chamber during Zr undersaturation (Corfu *et al.* 2003). As this process occurs during growth of the zircon it does not disturb the age information of the U–Pb system of the mineral, which reflects the magmatic event.

Another part of the Pelagonian Zone that is dominated by granites and gneisses is found about 80 km

Figure 6. (a) Geochronological results for Deskati orthogneiss Pl70 (single-zircon conventional U–Pb measurements). Error ellipses are 2σ. The light-coloured ellipses in the concordia diagram display inherited grains that were not included in the age calculation. (b) CL images showing typical internal structures of zircons.
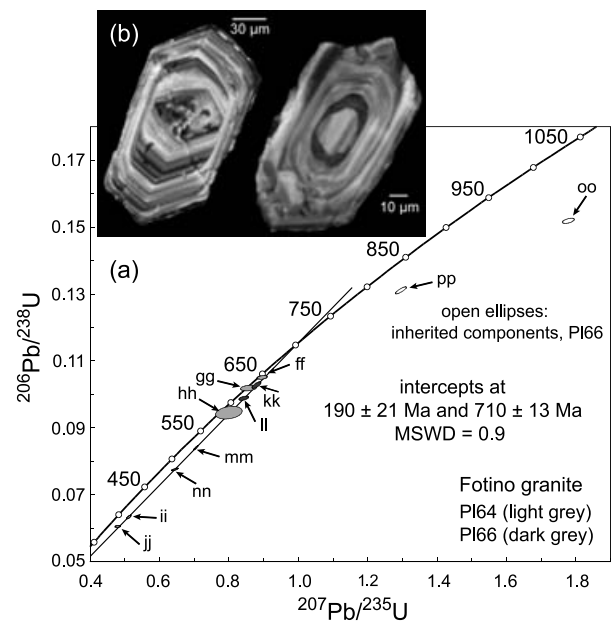

Figure 7. (a) Concordia diagram displaying the geochronological results for the Fotino granite (samples Pl64 and Pl66). Error ellipses are 2σ. The open error ellipses in the concordia diagram display inherited grains that were not included in the age calculation. (b) CL images of zircons from the Fotino granite showing a grain with a complex internal structure (left grain) and another with a rounded core (right grain).

SSE of Kastoria. Sample Pl70 is a coarse-grained orthogneiss that was taken near the eastern exit from Deskati village. It is a whitish gneiss that consists mainly of quartz, K-feldspar (partly sericitized), biotite, white mica, minor epidote and apatite. The orthogneiss was dated by the single-zircon U–Pb method. An upper intercept age of 699 ± 7 Ma (MSWD = 0.65) is interpreted as the emplacement age, while the scatter along the discordia is attributed to recent Pb loss (Fig. 6a). Two grains point to an older inherited component (grains dd and ee, Fig. 6a). Inherited components can be seen as rounded cores in some CL images. In the CL images, most zircons show irregular convolute structures in their centres (Fig. 6b). We interpret these domains as recrystallized areas. Pb loss is probably correlated with these domains and is most likely reflected in the discordance of the zircon grains. An interpretation of these areas as inherited components seems rather unlikely as such structures are abundant in CL images, while evidence for older components is far less evident in the U–Pb analyses.

The Fotino granite is exposed about 10 km further south of Deskati. Three samples of this granite were taken, two for geochronological purposes and one (Pl65) for geochemical analysis only. The Fotino granite is a pluton with variable deformation; sample Pl64 is a relatively strongly deformed variety of the Fotino granite and shows a gneissic texture, while sample Pl66 shows less deformation. The granites are medium-grained and have a greenish appearance. They differ only in their degree of deformation and have a main mineral composition of quartz, K-feldspar,

plagioclase, white mica, $\pm$ biotite, $\pm$ opaque phase and $\pm$ epidote. Tectono-metamorphism resulted in subgrain formation and partial recrystallization of K-feldspar, as well as secondary formation of white mica. For sample Pl64, dating by the conventional U–Pb method resulted in an upper intercept age of 685 ± 30 Ma (interpreted as the intrusion age) and a lower intercept age of 177 ± 31 Ma (MSWD = 0.68). Similar ages were obtained for the less deformed granite Pl66, that is, an upper intercept age of 706 ± 26 Ma and a lower intercept age of 178 ± 56 Ma (MSWD = 0.14). Moreover, two grains from this sample indicated an older inherited component. The ages of both Pl64 and Pl66 are subject to rather large errors but are identical within analytical error. Taken approximately two kilometres apart from each other along the road south of Fotino village, both samples belong to the same large plutonic body. We have therefore treated the two samples as one in a concordia diagram and extracted an upper intercept age of 710 ± 13 Ma (MSWD = 0.9), interpreted as the emplacement age of the Fotino pluton, and a lower intercept age of 190 ± 21 Ma (Fig. 7a). Internal structures of zircons in CL images (Fig. 7b) very much resemble those found in samples V9 and Pl70, with irregular domains at the centre of grains that otherwise show clear oscillatory zoning.

4. Geochemistry

Geochronology revealed two age groups, one with ages of approximately 300 Ma (samples V1 and Pl61) and

Table 4. Whole-rock XRF analyses

Location Rock	V1 Varnous granodiorite	V9 Varnous orthogneiss	Pl58 Florina orthogneiss	Pl59 Florina orthogneiss	Pl61 Kastoria granite	Pl70 Deskati orthogneiss	Pl64 Fotino granite	Pl65 Fotino granite	Pl66 Fotino granite
SiO_2	61.18	76.83	68.96	71.24	72.45	75.89	76.2	73.66	76.56
TiO_2	0.89	0.18	0.63	0.46	0.44	0.21	0.29	0.29	0.18
Al_2O_3	15.43	12.06	14.6	13.95	12.42	12.46	12.13	13.07	12.16
$Fe_2O_3^T$	5.34	1.33	4.09	3.00	3.54	1.40	1.41	1.81	1.23
MnO	0.10	0.02	0.05	0.03	0.07	0.02	0.01	0.02	0.02
MgO	3.11	0.15	1.38	0.76	1.19	0.24	0.24	0.27	0.15
CaO	4.44	0.25	1.64	1.24	1.66	0.60	0.30	0.60	0.41
Na_2O	3.38	2.77	2.34	2.68	2.46	2.69	2.73	2.98	3.05
K_2O	3.86	5.44	3.93	4.51	3.46	5.40	5.44	5.66	5.44
P_2O_5	0.48	0.03	0.15	0.11	0.19	0.04	0.05	0.05	0.03
LOI	0.98	0.42	1.87	1.18	1.50	0.60	0.58	0.68	0.62
Total	99.19	99.48	99.64	99.16	99.38	99.55	99.38	99.09	99.85
A/NK[1]	1.58	1.15	1.80	1.50	1.59	1.21	1.17	1.19	1.12
A/CNK[2]	0.87	1.11	1.32	1.21	1.15	1.10	1.11	1.08	1.04
Sc	13	5	7	5	7	4	3	3	3
V	112	9	64	42	51	14	13	17	9
Cr	69	6	24	16	26	6	4	3	4
Co	14	3	8	7	7	b.d.	3	3	3
Ni	37	5	9	8	9	b.d.	4	b.d.	3
Cu	3	4	8	7	2	3	9	3	3
Zn	64	20	57	41	49	26	22	29	34
Ga	17	14	17	16	16	14	16	16	14
Rb	138	233	117	142	161	213	245	302	248
Sr	806	36	152	125	572	63	37	42	35
Y	34	33	29	23	21	20	35	41	39
Zr	253	133	247	178	201	115	199	190	126
Nb	23	12	14	11	19	9	12	13	11
Ba	1291	277	985	877	590	371	186	206	257
Pb	13	16	19	16	14	17	35	17	24
Th	15	20	20	17	14	17	38	35	22
U	4	4	3	2	4	2	9	9	3

[1] A/NK: molecular ratio $Al_2O_3/(Na_2O + K_2O)$.
[2] A/CNK: molecular ratio $Al_2O_3/(CaO + Na_2O + K_2O)$.
b.d. below detection limit. $Fe_2O_3^T$: Fe expressed as total Fe_2O_3. Major element concentrations are given as wt%, trace element concentrations as ppm.
Analyses were performed with a Philips XRF at the Institut für Geowissenschaften, Universität Mainz, Germany.

another with ages of around 700 Ma (samples V9, Pl58/Pl59, Pl70, Pl64/66). The distinction between the two groups in terms of geochemistry and mineralogy is not as clear, though some slight differences are nevertheless apparent (Tables 4–6). These differences principally concern the presence of titanite and white mica in the rocks and the Sr and Eu content.

In regard to the mineralogy of the samples, it can be seen that titanite is a very common accessory mineral in the younger-age group; sample V1 in particular contains abundant titanite crystals with almost euhedral shape. By contrast, titanite was not observed in thin-sections in the older-age group, although Katerinopoulos, Kokkinakis & Kyriakopoulos (1996) reported fragments of anhedral titanite from the Fotino granite. Instead, the older rocks contain white mica that is absent from the younger ones. This difference indicates that the younger-age-group rocks show I-type granite characteristics while the older-age-group rocks are more akin to S-type granites.

According to their major-element chemistry, most of the rocks sampled are classified as granites (Fig. 8a; Table 4). Only sample V1 from the Varnous pluton plots in the granodiorite field in the normative Ab–An–Or classification diagram (O'Connor, 1965). This is due to its high CaO content of 4.44 wt %; all other samples have distinctly lower CaO concentrations.

Almost all samples are peraluminous with A/CNK values between 1.08 and 1.32, the only exception being granodiorite V1 which is classified as metaluminous with an A/CNK of 0.87. The A/NK values range from 1.12 to 1.80. Here, one can discriminate between the younger-age-group samples, together with orthogneisses Pl58 and Pl59 (A/NK = 1.50–1.80) and the remaining older-age-group samples (A/NK = 1.12–1.21).

A comparison of the geochemistry of the older-age-group rocks with that of Cadomian rocks from central Europe shows that both fall well within the same range, although an extensive comparison is hampered by the restricted range of SiO_2 encountered for the Pelagonian Zone samples, together with their limited sample number. Because the older-age-group rocks are characterized by high K_2O and Rb contents accompanied by low Na_2O, Sr and Ba contents, they are clearly different from M- or I-type plutons, such as

Table 5. Whole-rock laser-ablation ICP-MS analyses

Location Rock	V1 Varnous granodiorite	V9 Varnous orthogneiss	Pl58 Florina orthogneiss	Pl61 Kastoria granite	Pl70 Deskati orthogneiss	Pl64 Fotino granite	Pl66 Fotino granite
La	61.01	14.22	30.92	19.09	19.39	28.35	25.05
Ce	120.52	24.56	60.87	41.19	41.32	54.93	53.94
Pr	14.11	3.50	7.81	5.53	4.78	6.57	6.02
Nd	52.13	12.57	30.18	21.74	16.93	22.22	21.32
Sm	8.88	2.56	6.05	4.14	2.97	4.08	4.28
Eu	2.08	0.18	1.06	0.96	0.41	0.40	0.32
Gd	7.12	2.58	5.52	3.47	2.50	3.64	4.04
Tb	0.95	0.46	0.80	0.50	0.39	0.59	0.71
Dy	5.33	3.17	4.66	2.90	2.55	3.67	4.66
Ho	0.98	0.67	0.88	0.54	0.53	0.74	0.96
Er	2.73	2.10	2.45	1.65	1.59	2.21	2.93
Tm	0.40	0.32	0.35	0.25	0.25	0.33	0.45
Yb	2.78	2.29	2.34	1.74	1.78	2.35	3.16
Lu	0.41	0.34	0.35	0.26	0.26	0.35	0.46
Hf	7.05	2.50	6.44	4.86	3.16	4.05	3.04
Ta	1.37	0.78	0.96	1.33	0.80	0.93	1.11
Eu/Eu^*	0.80	0.21	0.56	0.77	0.46	0.32	0.24
$(La/Yb)_n$	14.80	4.19	8.91	7.39	7.34	8.14	5.34

$_n$ Normalized to chondrite.

Analyses were performed on molten samples with a Finnigan Element 2 at the Max-Planck-Institut für Chemie, Mainz, Germany; sample preparation followed Gumann, Lahaye & Brey (2003). Concentrations given as ppm.

Table 6. Whole-rock isotope composition data

	Location	Age (Ma)	$^{143}Nd/^{144}Nd_m$	$\pm 2\sigma$	$^{147}Sm/^{144}Nd^2$	$^{143}Nd/^{144}Nd_i$	εNd_i	T_{DM}^4 (Ga)	$^{87}Sr/^{86}Sr_m$	$\pm 2\sigma$	$^{87}Rb/^{86}Sr^3$	$^{87}Sr/^{86}Sr_i$
V1	Varnous	298	0.512357	9	0.1032	0.512156	−1.9	1.0	0.707395	11	0.5	0.70529
V9	Varnous	713	0.512195	4	0.1233	0.511619	−2.0	1.5	0.869376	12	19.0	< 0.7000
Pl58	Florina	710	0.512041	8	0.1214	0.511476	−4.8	1.7	0.733084	14	2.2	0.71046
Pl61	Kastoria	292	0.512272	8	0.1153	0.512052	−4.1	1.2	0.711694	6	0.8	0.70831
Pl70	Deskati	699	0.512089	8	0.1062	0.511602	−2.6	1.4	0.801525	16	9.9	0.70305
Pl64	Fotino	710	0.512299	23	0.1112	0.511781	1.2	1.2	0.859820	19	19.4	< 0.7000
Pl64$_d$	Fotino	710	0.512285	8	0.1112	0.511767	0.9	1.2	0.863401	18	19.5	< 0.7000
Pl66	Fotino	710	0.512177	8	0.1216	0.511611	−2.2	1.5	0.898412	19	20.9	< 0.7000

[1] $^{143}Nd/^{144}Nd_m$ corrected to an average La Jolla of 0.511823.
[2] $^{147}Sm/^{144}Nd$ calculated with concentrations by laser-ablation ICP-MS (Table 5).
[3] $^{87}Rb/^{86}Sr$ calculated with concentrations by XRF analyses (Table 4).
[4] Depleted mantle values from Michard *et al.* (1985).
$_d$ Duplicate analysis.

the North Tregor Batholith of NW France (Graviou & Auvray, 1990), but similar to Cadomian granitoids with hybrid to S-type characteristics.

Applying the trace-element discrimination diagrams of Pearce, Harris & Tindle (1984), a syn-collisional or volcanic-arc origin of the sampled rocks is indicated (Fig. 8b). Only sample V1 plots slightly inside the within-plate granite field, which might be an indication for a late- or post-collisional origin.

The chondrite-normalized REE patterns are typical of rocks formed in a volcanic-arc or active continental margin setting (Fig. 9). Light REE are enriched while the heavy REE display a flat pattern. A clear distinction between the older- and the younger-age-group rocks can be seen in the Eu anomaly, which is more pronounced in the older-age-group rocks (Eu/Eu* is between 0.21 and 0.56 as opposed to values of 0.80 and

0.77 for the younger-age-group rocks). Granodiorite V1 shows the largest enrichment of LREE with a $(La/Yb)_n$ of about 15, while for the remainder of the samples this ratio is in the range of 4 to 9.

The Nd-isotope composition analyses resulted in εNd_i values of between +0.9 and −4.8 for the older-age-group rocks (Table 6), and between −1.9 and −4.1 for the younger-age-group rocks. This parameter cannot, therefore, discriminate between the two age groups. The same holds true for the depleted-mantle model ages (T_{DM}), which ideally date the time of crust-mantle differentiation but normally reflect the average age of mixed crustal and mantle components that participated in magma genesis (Arndt & Goldstein, 1987). The T_{DM} (1.2 Ga) value for Kastoria granite Pl61 is older than that of granodiorite V1 (1.0 Ga) and its εNd_i more negative. This might suggest that
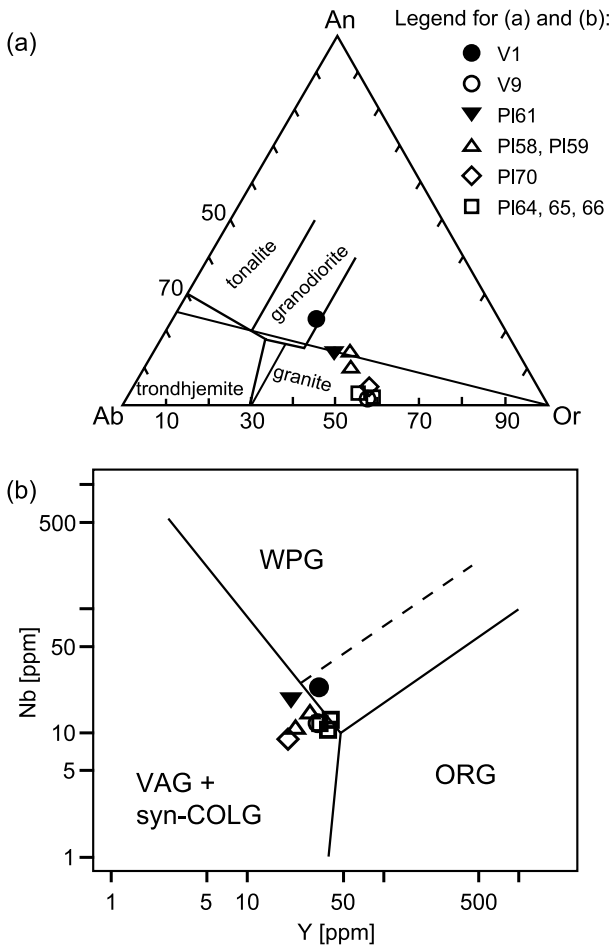
Figure 8. Geochemical classification of the analysed rocks. (a) The normative Ab–An–Or classification diagram of O'Connor (1965), modified by Barker (1979, heavy lines). (b) Geotectonic-environment classification after Pearce, Harris & Tindle (1984); WPG – within-plate granite; ORG – ocean ridge granite; VAG – volcanic arc granite; syn-COLG – syn-collisional granite.
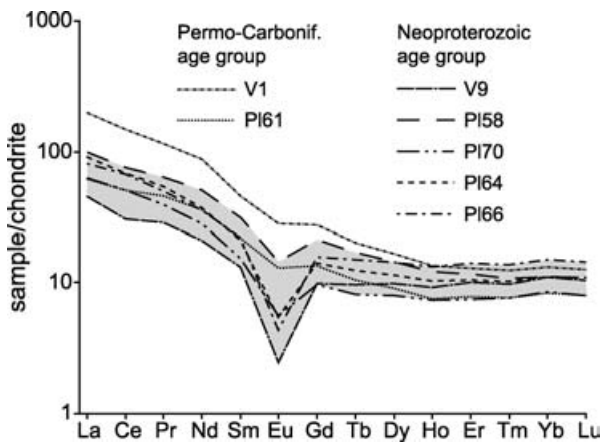

Figure 9. Chondrite-normalized REE patterns (chondrite values from Boynton, 1984). Note the pronounced negative Eu-anomaly in the pattern of the Neoproterozoic gneisses (grey area) in comparison to the Carboniferous samples.

the crustal component involved in magma genesis for Kastoria granite Pl61 was either larger or older than that for V1. The difference in εNd_i and T_{DM} for the samples from the Fotino granite could reflect heterogeneity within the pluton, possibly related to the assimilation of varying amounts of older crustal material. Of the older-age-group rocks, orthogneiss Pl58 shows the most negative εNd_i value (-4.8) and the oldest T_{DM} value (1.7 Ga). These values indicate the involvement of a large crustal component and therefore a clear S-type character for the protolith of orthogneiss Pl58, which is further confirmed by the abundance of rounded zircon cores that can be seen in CL images.

Contrary to the Nd-isotope system, which is unlikely to be disturbed by later thermal events (DePaolo, 1981), the Sr isotope system is more readily affected by metamorphism or alteration. Strontium isotope composition analyses clearly show that the Rb–Sr system, at least of the Neoproterozoic rocks from Fotino (Pl64, Pl66) and Varnous (V9), is disturbed (Table 6). This is indicated by the high $^{87}Rb/^{86}Sr$ values (~ 20) and the unrealistically low $^{87}Sr/^{86}Sr_i$ values (< 0.7000). Such exceptionally low $^{87}Sr/^{86}Sr_i$ values could be an effect of overcorrection due to small errors in Sr concentration measurements and resultant Rb–Sr ratios, as slight changes of very high Rb–Sr ratios significantly affect the initial ratios. Alternatively, they could be related to either secondary Sr loss or Rb gain. The rather low Sr content (~ 40 ppm) of the samples with unrealistically low $^{87}Sr/^{86}Sr_i$ values correlates with low Ca concentrations and large negative Eu anomalies; the low Sr concentration could therefore be a primary feature related to plagioclase fractionation. On the other hand, recrystallization of primary and/or formation of secondary white mica as well as recrystallization of K-feldspar might be responsible for elevated Rb concentrations. It is worth noting that the Neoproterozoic rocks that yielded the unrealistically low $^{87}Sr/^{86}Sr_i$ values are the ones with the strongest evidence for metamorphic overprint in the form of recrystallized microcline and formation of secondary muscovite. This might indicate that the high concentration of Rb and low concentration of Sr observed is influenced by alteration processes accompanying deformation. An increase of the Rb/Sr due to alteration would consequently result in $^{87}Sr/^{86}Sr_i$ values which are too low. Thus, the $^{87}Sr/^{86}Sr_i$ values we obtained are minimum values. In any case, the $^{87}Sr/^{86}Sr_i$ value of 0.70529 for granodiorite V1 concurs with that of ~ 0.7056 reported by Koroneos *et al.* (1993) from the Varnous pluton. It indicates the dominance of mantle material as the source material, with only small amounts of older crustal material being involved. Kastoria granite Pl61 has a higher $^{87}Sr/^{86}Sr_i$ of 0.70831, implying a larger amount of crustal component in the source, as already deduced from the Nd isotopes. The rather high $^{87}Sr/^{86}Sr_i$ of 0.71046 for orthogneiss

Pl58 underlines its derivation from an S-type granite involving older crustal material.

5. Discussion

The geochronological, geochemical and Sr- and Nd-isotope results of this study shed new light on our knowledge of the Pelagonian Zone. The picture of a single Permo-Carboniferous basement for this zone should be modified to include the existence of a second, distinctly older basement of Neoproterozoic age, identified here for the first time.

5.a. Permo-Carboniferous rocks

The Permo-Carboniferous ages of 298 ± 7 Ma for granodiorite V1 from the Varnous Mountains and of 292 ± 5 Ma for Kastoria granite Pl61 are zircon ages typical of the basement rocks from the Pelagonian Zone that have been studied to date (e.g. Yarwood & Aftalion, 1976; Mountrakis, 1984; Koroneos *et al.* 1993; Vavassis *et al.* 2000; Reischmann *et al.* 2001; Anders *et al.* 2003).

5.b. Neoproterozoic basement rocks

5.b.1. Neoproterozoic ages

Neoproterozoic ages of basement rocks in the NW Pelagonian Zone are in the range of 699 to 713 Ma. Because of this rather short time span and the fact that they are largely identical within analytical error, one may assume that the rocks formed during a single major magmatic event in the Neoproterozoic. The Neoproterozoic basement rocks of the Pelagonian Zone are the oldest known rocks from Greece.

5.b.2. Post-emplacement processes

Due to the igneous zoning of the zircons of the Neoproterozoic rocks, the ages obtained are interpreted as magmatic crystallization ages. Some of the zircons show evidence of Pb loss during a secondary overprint. Pb loss can be interpreted as recent only in the case of Deskati orthogneiss Pl70. For both samples from the Fotino granite and the orthogneiss from the Varnous Mountains (V9), the lower intercepts are at 190 ± 21 Ma and 187 ± 59 Ma, respectively (if the two samples from the Fotino granite are considered separately, the resulting lower intercepts are at 177 ± 31 Ma and 178 ± 56 Ma). The geological meaning of these lower intercept ages is not yet clear. Lead loss in zircons is a common phenomenon and mostly attributed to metamictization and later recrystallization during which Pb is removed from the zircon crystal (Williams, 1992; Mezger & Krogstad, 1997). This Pb loss can occur either during distinct episodic events or continuously over a large time period, something which is not obvious from the concordia diagram but which

will lead to different results. In general, lower intercept ages do not necessarily have a geological meaning and therefore have to be handled with care (Mezger & Krogstad, 1997). In the case of the rocks from the NW Pelagonian Zone, a link between the lower intercept ages and regional geology might be suggested when comparing them to ages proposed for the spreading and obduction of the Pindos and Vourinos ophiolites. Liati, Gebauer & Fanning (2004) dated zircons from gabbros and a plagiogranite from the Pindos and Vourinos ophiolites using SHRIMP, and obtained ages in the range of 169 ± 2 Ma to 173 ± 3 Ma. Ar–Ar dating of amphibole from the metamorphic sole of the Vourinos ophiolite yielded an age of about 171 ± 4 Ma (Spray *et al.* 1984). However, today at least, the above ophiolites crop out several kilometres away from our sampling positions and there is no definitive proof that spreading or obduction of the ophiolites could have affected the isotopic system of our samples. Mountrakis (1982, 1984, 1986) recognized polyphase deformation in the NW Pelagonian Zone and suggested a pre-Upper Carboniferous and an Upper Jurassic age for the two oldest deformation phases. However, we see no convincing link between ophiolite obduction and a regional metamorphic overprint, therefore an attribution of the lower intercept ages to unspecific, episodic Pb loss seems more appropriate. This Pb loss is probably related to thermal/metamorphic events that affected the Pelagonian Zone during Latest Jurassic, Cretaceous and Tertiary times (e.g. Schermer, Lux & Burchfiel, 1990; Most, 2003).

With regard to the Fotino granite, overprinting by a post-Neoproterozoic event is evident. Katerinopoulos, Kokkinakis & Kyriakopoulos (1996) dated white micas and whole-rock from the Fotino granite by the Rb–Sr method and obtained ages in the range of 225 to 273 Ma. The above authors interpret the older ages as intrusion ages and explain the younger ages as Rb–Sr open-system behaviour. The disturbance of the Rb–Sr system of most of the Neoproterozoic rocks, including the Fotino granite, is also evident from the unrealistically low $^{87}Sr/^{86}Sr_i$ values of < 0.7000 (Table 6). Therefore, in the light of the new zircon ages and Sr isotope measurements of our study, all Rb–Sr ages of Katerinopoulos, Kokkinakis & Kyriakopoulos (1996) reflect, at best, a thermal event that occurred between Late Permian and Jurassic times. This thermal event is probably reflected in the lower intercept ages of the zircons from the Fotino granite.

It is noteworthy that the Neoproterozoic zircons do not appear to have been influenced by a Permo-Carboniferous thermal event, despite the fact that this time span is characterized by widespread magmatism. This indicates that the Neoproterozoic rocks sampled did not experience temperatures high enough during Permo-Carboniferous times to affect the U–Pb system of the zircon grains. Whether the absence of a Permo-Carboniferous overprint is a general feature of the

Neoproterozoic rocks from the Pelagonian Zone or a consequence of the still-small database will be a matter for future research.

5.c. Derivation and possible linkages of the Pelagonian Neoproterozoic rocks

The Neoproterozoic zircon ages of 699 Ma to 713 Ma are the oldest ages of basement rocks known from Greece. Basement rocks with intrusion ages of about 700 Ma are not known from the neighbouring Hellenide zones. Traditionally, the tectonostratigraphic zones of the Hellenides are correlated with those of Turkey (e.g. S. Dürr, unpub. Habilitations thesis, Univ. Marburg, 1975; Jacobshagen, 1986). Zircon dating of granitoid basement from adjacent zones in Turkey so far yielded only Late Neoproterozoic ages of *c*. 520 to 590 Ma for the Menderes Massif (Hetzel & Reischmann, 1996; Loos & Reischmann, 1999; Gessner *et al.* 2004) and also for the Karadere basement from the Istanbul Zone, NW Turkey (Chen *et al.* 2002). The large difference in ages observed does not support a correlation of the Pelagonian Zone Neoproterozoic basement with either the Menderes Massif or the Karadere basement.

The spatial distribution of the Neoproterozoic rocks in the Pelagonian Zone is not yet accurately known. As our samples were taken several tens of kilometres apart (distributed over an area of about 20×100 kilometres), only inferences can be made about their possible contiguity in Neoproterozoic times. Their strong chemical and mineralogical similarities suggest that they once belonged to a single basement unit that was later dissected by Variscan and Alpine tectonomagmatic events. These old basement rocks are interpreted to be remnants of a terrane, which we call here the Florina Terrane, which constituted the continental crust on which the Pelagonian Permo-Carboniferous magmatic arc was built.

The ages yielded (*c*. 700 Ma) support the argument that the Florina Terrane originated in Gondwana but not in Baltica. Neoproterozoic ages of approximately 700 Ma are known from Pan-African Gondwana-derived terranes like West and East Avalonia or the Armorica Terrane Assemblage; they mark an era of widespread subduction-related magmatism along or close to the northern margin of Gondwana. Later, rifting of this Pan-African magmatic arc along the northern margin of Gondwana led to the detachment and dispersal of the terranes. Today these terranes can be found in NE North America (West Avalonia) and in the Variscides of Europe (East Avalonia and the Armorica Terrane Assemblage). Palaeo-reconstructions place the Avalonia terranes in the western part of the Pan-African magmatic arc and the Armorica terranes further east (e.g. Nance & Murphy, 1994).

Inferences as to which part of the northern margin of Gondwana the Florina Terrane of the Pelagonian Zone comes from can be made by comparing Nd-isotope systematics and the provenance of detrital zircons of these different terrane assemblages, as they display distinct differences. Nd-isotope systematics reveal the characteristics of the source from which the magma is derived (including the contribution of older crustal material). The distribution of ages of inherited zircons, on the other hand, points to the age of the contributing crustal source rocks and the exposed cratons nearby.

5.c.1. Comparison of the Florina Terrane with West Avalonia

Ages of about 700 Ma are known from both West and East Avalonia, where an early phase of arc-related magmatism is recognized between 780 and 660 Ma (Murphy *et al.* 1999 and references therein). A compilation of data by Nance & Murphy (1996) and Murphy & Nance (2002) reveals that West Avalonia terranes tend to display immature arc characteristics with predominantly positive εNd_i (for Neoproterozoic felsic volcanics it ranges from $+0.8$ to $+3.0$) and Nd model ages T_{DM} between 0.9 and 1.2 Ga. The εNd_i values of the Neoproterozoic rocks from the Florina Terrane differ in that they range from about $+0.9$ to -2.6. Orthogneiss Pl58, which has a strong sedimentary character, shows an even more negative εNd_i value of -4.8. The depleted mantle model ages for the Florina Terrane are also somewhat older than those for West Avalonia, varying mostly between 1.2 and 1.5 Ga. Detrital zircon ages from West Avalonia are distributed over several distinct age groups of about 1.0–1.2 Ga (Grenvillian), 1.5–1.8 Ga, 2.0–2.1 Ga and 2.6 Ga (e.g. Keppie, Davis & Krogh, 1998). Several workers (e.g. Keppie, Davis & Krogh, 1998; Murphy & Nance, 2002; Nance & Murphy, 1994) pointed out that these age groups correspond to age groups known from the Amazonian craton, while at the same time a derivation from NW Africa seems unlikely because ages in the range of 1.0–1.8 Ga are virtually absent from this craton. Therefore, the presence of Grenvillian and older Mesoproterozoic detrital zircon ages implies that West Avalonia originated either adjacent to the Amazonia/South America craton or at least close enough to receive its characteristic detrital zircon assemblage (e.g. Nance & Murphy, 1994; Keppie, Davis & Krogh, 1998; McNamara *et al.* 2001). As for the Florina Terrane of the NW Pelagonian Zone, the Neoproterozoic samples taken as a whole give the following picture. An Early Mesoproterozoic component is evident in both a $^{207}Pb/^{206}Pb$ age of 1777 Ma from Varnous orthogneiss V9 (grain V9-C, Table 1) and in a SHRIMP analysis of a zircon core from orthogneiss Pl58 from which a concordant $^{206}Pb/^{238}U$ age of 1501 ± 9 Ma was obtained (Pl58 spot 3.2, Table 3). All other $^{207}Pb/^{206}Pb$ ages from samples V9, Pl58, Pl59, Pl70 and Pl66 range from *c*. 800 to 1340 Ma. It should be noted that $^{207}Pb/^{206}Pb$ ages in
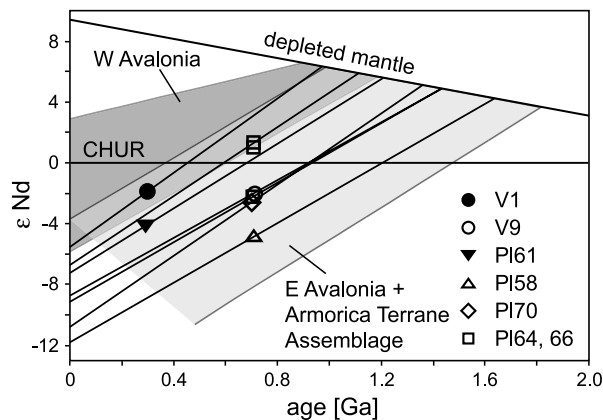
Figure 10. Neodymium-isotope evolution for the basement rocks of the NW Pelagonian Zone. Depleted-mantle evolution line is after Michard *et al.* (1985). Shown for comparison are the fields for West Avalonia (light grey area) and East Avalonia plus Armorica Terrane Assemblage rocks (dark grey area), redrawn from Murphy & Nance (2002). CHUR – chondritic uniform reservoir.

the range of 850 to 1150 Ma might indicate a relation to the Grenvillian orogeny. By definition, ^{207}Pb/^{206}Pb ages are minimum ages and display the 'true' age only if they are concordant. Looking at the concordia diagrams, all of the grains with inherited components are discordant to varying degrees and therefore the 'true' ages of the protoliths are likely to be older; how much older, however, cannot be said. Assuming that this range of ^{207}Pb/^{206}Pb ages reflects a Late Neoproterozoic to Mesoproterozoic source, an affinity of the Florina Terrane to Avalonia is indicated by the detrital zircon ages, though not necessarily by the Nd isotopes.

5.c.2. *Comparison of the Florina Terrane with East Avalonia*

East Avalonia shows a range of Neoproterozoic magmatic ages similar to that of West Avalonia. What distinguishes East from West Avalonia is the range of εNd$_i$ values for the late Neoproterozoic to Cambrian igneous and sedimentary rocks (-2.0 to -8.5), although rocks with εNd$_i$ values up to $+4.6$ have been reported (Davies, Gledhill & Hawkesworth, 1985; Thorogood, 1990), the latter resembling West Avalonia lithologies. Depleted-mantle model ages for East Avalonia are slightly older than those for West Avalonia and are in the order of 1.0 to 1.8 Ga (Davies, Gledhill & Hawkesworth, 1985; Thorogood, 1990). Comparison between East Avalonia and Florina shows good agreement in Nd isotopes (Fig. 10). East Avalonia is interpreted by Nance & Murphy (1996) and Murphy & Nance (2002) to have originated in a region along the northern margin of Gondwana that is neither entirely Amazonia-related nor NW-Africa-related, but consists of reworked material of both Amazonia-type and NW-Africa-type crust.

5.c.3. *Comparison of the Florina Terrane with the Armorica Terrane Assemblage*

The Armorica Terrane Assemblage is characterized by basement intrusion ages of about 560–580 Ma (Linnemann *et al.* 2000), although older zircon ages of about 650–670 Ma do exist, for example, from orthogneiss boulders of the Cesson conglomerate (North Brittany, France: Guerrot & Peucat, 1990), and indicate the presence of the same Neoproterozoic magmatic phase that is known from Avalonia. With predominantly negative εNd$_i$ values ($+1.6$ to -9.9) and T$_{DM}$ values of 1.0 to 1.7 (D'Lemos & Brown, 1993), the Late Precambrian–Cambrian Armorica Terrane Assemblage basement rocks show a strong similarity to those known from East Avalonia and the Florina Terrane. However, Mesoproterozoic detrital zircon ages are so far unknown from the Armorica Terrane Assemblage, where Palaeoproterozoic and Archaean ages predominate (e.g. Linnemann *et al.* 2000). The absence of Early to Late Mesoproterozoic detrital zircon ages coupled with the presence of Palaeoproterozoic and Archaean detrital zircons favours a derivation of the Armorica Terrane Assemblage from close to NW Africa (e.g. Nance & Murphy, 1996; Linnemann *et al.* 2000; Murphy & Nance, 2002). Despite the similarity in Nd isotopes, the Florina Terrane and the Armorica Terrane Assemblage are clearly different in terms of the distribution of detrital zircon ages.

5.c.4. *Comparison of the Florina Terrane with the Arabian–Nubian Shield*

Neoproterozoic intrusion ages of about 700 Ma are also known from NE Africa and Arabia, especially the Eastern Desert of Egypt, Sinai, Israel, Sudan (Arabian–Nubian Shield) and Ethiopia (e.g. Kröner, Krüger & Rashwan, 1994; Teklay *et al.* 1998; Bregar *et al.* 2002; Meert, 2003 and references therein). However, an origin of the Florina Terrane from close to Arabia seems unlikely since geochemical analyses indicate formation of large parts of the Arabian–Nubian Shield in an oceanic volcanic-arc setting during Neoproterozoic times (e.g. Kröner *et al.* 1991).

5.c.5. *Avalonia terranes in the Variscide orogeny*

We conclude that an affinity of the Florina Terrane to Avalonia is supported by the Mesoproterozoic ^{207}Pb/^{206}Pb ages of inherited zircons. The existence of a Mesoproterozoic detrital component does not support either a correlation of the Florina Terrane with the Armorica Terrane Assemblage or a derivation from NE Africa and Arabia. A distinction between West and East Avalonia can be made on the basis of Nd-isotope analyses; they suggest an East Avalonian affinity for the Florina Terrane.

In a simplified view, in Europe the northern Variscides comprise East Avalonia terranes (Gibbons & Horák, 1996 and references therein), whereas the southern Variscides comprise the Armorica Terrane Assemblage (Tait *et al.* 1997). The Florina Terrane of East Avalonian affinity lies south of the Armorica Terrane Assemblage and does not fit the pattern of terrane distribution in the Variscides described above. However, this simple pattern was questioned in the eastern Variscides (Bohemia: Finger *et al.* 2000), where the basement of the Moravo-Silesicum was re-interpreted as an Avalonia-type terrane on the basis of Nd-isotope systematics (Hegner & Kröner, 2000) and detrital zircon dating by SHRIMP (Friedl *et al.* 2000). A basement gneiss of the Silesian domain was dated by the single-zircon Pb–Pb evaporation method at about 685 Ma (Kröner *et al.* 2000). It thus seems plausible that the Neoproterozoic basement of the Pelagonian Zone formed in a similar way to the terranes of the Variscides. Although the Palaeozoic evolution of these Gondwana-derived terranes is different, they nevertheless became involved in the same Permo-Carboniferous orogenic processes that took place at the southern margin of Europe. Geochemical analyses indicate a volcanic-arc or active continental-margin setting for the Permo-Carboniferous magmatism of the Pelagonian Zone (see also Pe-Piper, Doutsos & Mijara, 1993; Pe-Piper, Doutsos & Mporonkay, 1993; Katerinopoulos *et al.* 1998; Anders *et al.* 2003). These rocks might therefore be compared to the pre-alpine I-type granitoids of the Alps, which were interpreted by Finger & Steyrer (1990) to have originated at the South European margin in the course of northward subduction of (a branch of) the Palaeotethys. The alpine tectono-metamorphic overprint onto the Pelagonian Zone basement rocks, however, impedes a direct correlation with this Palaeozoic belt in the Alps.

The discovery of the Florina Terrane and its interpretation as a Gondwana-derived terrane, most probably belonging to East Avalonia, underlines the characterization of the evolutionary history of the Eastern Mediterranean by arc-accretion processes.

6. Conclusions

New information that is essential for unravelling the Late Neoproterozoic–Palaeozoic evolutionary history of the eastern Mediterranean area is presented in this study.

The geochronological and geochemical results support the notion that the pre-alpine basement of the Pelagonian Zone in Greece formed in at least two distinct episodes. The new zircon ages of basement gneisses and granites document the existence of Neoproterozoic crustal rocks in the northwestern part of the Pelagonian Zone in addition to the well-known Permo-Carboniferous basement rocks.

Trace-element geochemistry suggests formation of basement rocks of both age groups in an active continental margin or volcanic-arc setting.

The Neoproterozoic ages of *c*. 699 Ma to 713 Ma for the older-age-group rocks are the oldest recorded ages to this date from the Pelagonian Zone and from Greece in general.

For the Neoproterozoic basement rocks from the Pelagonian Zone, the existence of inherited zircons with Mesoproterozoic minimum ages and Mesoproterozoic Nd model ages suggests formation at or close to the continental margin of northern Gondwana. These Neoproterozoic rocks are interpreted as remnants of a Gondwana-derived terrane, named here the Florina Terrane.

Geochronological analyses and Nd isotopes indicate a similarity of the Florina Terrane to Avalonia-type terranes, therefore a derivation similar to that of East Avalonia is suggested.

The Florina Terrane forms the continental basement on which the Pelagonian Permo-Carboniferous magmatic arc formed and was later incorporated in the Hellenide orogen.

References

ANDERS, B., REISCHMANN, T., POLLER, U. & KOSTOPOULOS, D. 2003. First zircon ages from South Pilion and Skiathos Island, Greece. *Berichte der Deutschen Mineralogischen Gesellschaft, Beiheft zum European Journal of Mineralogy* **15/1**, 5.

ARNDT, N. T. & GOLDSTEIN, S. L. 1987. Use and abuse of crust-formation ages. *Geology* **15**, 893–5.

AUBOUIN, J., BRUNN, J. H., CELET, P., DERCOURT, J., GODFRIAUX, I. & MERCIER, J. 1963. Esquisse de la Géologie de la Grèce. *Livre Mémoire Professeur Fallot, Mémoires Société géologique de France*, 383–610.

BARKER, F. 1979. Trondhjemite: Definition, environment and hypotheses of origin. In *Trondhjemites, dacites and related rocks* (ed. F. Barker), pp. 1–12. Amsterdam: Elsevier.

BLACK, L. P., KAMO, S. L., ALLEN, C. M., ALEINIKOFF, J. N., DAVIS, D. W., KORSCH, R. J. & FOUDOULIS, C. 2003. TEMORA 1: a new zircon standard for Phanerozoic U–Pb geochronology. *Chemical Geology* **200**, 155–70.

BOYNTON, W. V. 1984. Cosmochemistry of the rare earth elements: meteorite studies. In *Rare Earth Element Geochemistry* (ed. P. Henderson), pp. 63–114. Amsterdam: Elsevier.

BREGAR, M., BAUERNHOFER, A., PELZ, K., KLOETZLI, U., FRITZ, H. & NEUMAYR, P. 2002. A late Neoproterozoic magmatic core complex in the Eastern Desert of Egypt:

emplacement of granitoids in a wrench-tectonic setting. *Precambrian Research* **118**, 59–82.

CHEN, F., SIEBEL, W., SATIR, M., TERZIOGLU, M. N. & SAKA, K. 2002. Geochronology of the Karadere basement (NW Turkey) and implications for the geological evolution of the Istanbul Zone. *International Journal of Earth Sciences* **91**, 469–81.

CHERNIAK, D. J. & WATSON, E. B. 2000. Pb diffusion in zircon. *Chemical Geology* **172**, 5–24.

CONNELLY, J. N. 2000. Degree of igneous zonation in zircon as a signpost for concordancy in U/Pb geochronology. *Chemical Geology* **172**, 25–39.

CORFU, F., HANCHAR, J. M., HOSKIN, P. W. O. & KINNY, P. 2003. Atlas of zircon textures. In *Zircon* (eds J. M. Hanchar and P. W. O. Hoskin), pp. 468–500. Reviews in Mineralogy and Geochemistry no. 53.

DAVIES, G., GLEDHILL, A. & HAWKESWORTH, C. 1985. Upper crustal recycling in southern Britain: evidence from Nd and Sr isotopes. *Earth and Planetary Science Letters* **75**, 1–12.

DEPAOLO, D. J. 1981. Neodymium isotopes in the Colorado Front Range and crust-mantle evolution in the Proterozoic. *Nature* **291**, 193–6.

D'LEMOS, R. S. & BROWN, M. 1993. Sm–Nd isotope characteristics of late Cadomian granite magmatism in northern France and the Channel islands. *Geological Magazine* **130**, 797–804.

ENGEL, M. & REISCHMANN, T. 1998. Single-zircon Geochronology of the orthogneisses from Paros, Greece. *Bulletin of the Geological Society of Greece* **XXXII/3**, 91–9.

FINGER, F. & STEYRER, H. P. 1990. I-type granitoids as indicators of a late Paleozoic convergent ocean-continent margin along the southern flank of the central European Variscan orogen. *Geology* **18**, 1207–10.

FINGER, F., HANŽL, P., PIN, C., VON QUADT, A. & STEYRER, H. P. 2000. The Brunovistulian: Avalonian Precambrian sequence at the eastern end of the Central European Variscides? In *Orogenic Processes: Quantification and Modelling in the Variscan Belt* (eds W. Franke, V. Haak, O. Oncken and D. Tanner), pp. 103–12. Geological Society of London, Special Publication no. 179.

FRIEDL, G., FINGER, F., MCNAUGHTON, N. J. & FLETCHER, I. R. 2000. Deducing the ancestry of terranes: SHRIMP evidence for South America derived Gondwana fragments in central Europe. *Geology* **28**, 1035–8.

GESSNER, K., COLLINS, A. S., RING, U. & GÜNGÖR, T. 2004. Structural and thermal history of poly-orogenic basement: U-P geochronology of granitoid rocks in the southern Menderes Massif, Western Turkey. *Journal of the Geological Society, London* **161**, 93–101.

GIBBONS, W. & HORÁK, J. M. 1996. The Evolution of the Neoproterozoic Avalonian Subduction System: Evidence from the British Isles. In *Avalonia and related peri-Gondwana terranes of the circum-North Atlantic* (eds R. D. Nance and M. D. Thompson), pp. 269–80. Geological Society of America, Special Paper no. 304.

GRAVIOU, P. & AUVRAY, B. 1990. Late Precambrian M-type granitoid genesis in the Cadomian belt of NW France. In *The Cadomian orogeny* (eds R. S. D'Lemos, R. A. Strachan and C. G. Topley), pp. 231–44. Geological Society of London, Special Publication no. 51.

GUERROT, C. & PEUCAT, J. J. 1990. U–Pb geochronology of the Upper Proterozoic Cadomian orogeny in the northern Armorican Massif, France. In *The Cadomian*

orogeny (eds R. S. D'Lemos, R. A. Strachan and C. G. Topley), pp. 13–26. Geological Society of London, Special Publication no. 51.

GUMANN, S., LAHAYE, Y. & BREY, G. P. 2003. Iridium-Strip – Rhyolite enthüllen ihre Details. *Berichte der Deutschen Mineralogischen Gesellschaft, Beiheft zum European Journal of Mineralogy* **15/1**, 72.

HEGNER, E. & KRÖNER, A. 2000. Review of Nd isotopic data and xenocrystic and detrital zircon ages from the pre-Variscan basement in the eastern Bohemian Massif: speculations on palinspastic reconstructions. In *Orogenic Processes: Quantification and Modelling in the Variscan Belt* (eds W. Franke, V. Haak, O. Oncken and D. Tanner), pp. 113–29. Geological Society of London, Special Publication no. 179.

HETZEL, R. & REISCHMANN, T. 1996. Intrusion age of Pan-African augen gneisses in the southern Menderes Massif and the age of cooling after Alpine ductile extensional deformation. *Geological Magazine* **133**, 565–72.

IGME. 1983. *Geological Map of Greece, scale 1:500 000.* Institute of Geology and Mineral Exploration.

JACOBSHAGEN, V. 1986. *Geologie von Griechenland.* Berlin/Stuttgart: Gebrueder Borntraeger, 363 pp.

KATERINOPOULOS, A., KOKKINAKIS, A. & KYRIAKOPOULOS, K. 1996. Mineralogy, Petrology and Geochemistry of the Fotino Granitic Rocks, Thessaly, Central Greece. *Slovak Geological Magazine* **2**, 87–101.

KATERINOPOULOS, A., KYRIAKOPOULOS, K., DEL MORO, A., KOKKINAKIS, A. & GIANNOTTI, U. 1998. Petrology, Geochemistry and Rb/Sr Age Determination of Hercynian Granitic Rocks from Thessaly, Central Greece. *Chemie der Erde* **58**, 64–79.

KEPPIE, J. D., DAVIS, D. W. & KROGH, T. E. 1998. U–Pb geochronological constraints on Precambrian stratified units in the Avalon Composite Terrane of Nova Scotia, Canada: tectonic implications. *Canadian Journal of Earth Sciences* **35**, 222–36.

KOBER, B. 1986. Whole grain evaporation for ^{207}Pb/^{206}Pb-age investigations on single zircons using a double filament thermal ion source. *Contributions to Mineralogy and Petrology* **93**, 482–90.

KOBER, B. 1987. Single-zircon evaporation combined Pb + emitter-bedding for ^{207}Pb/^{206}Pb-age investigations using thermal ion mass spectrometry, and applications to zirconology. *Contributions to Mineralogy and Petrology* **96**, 63–71.

KORONEOS, A., CHRISTOFIDES, G., DEL MORO, A. & KILIAS, A. 1993. Rb–Sr geochronology and geochemical aspects of the Eastern Varnountas plutonite (NW Macedonia, Greece). *Neues Jahrbuch für Mineralogie, Abhandlungen* **165/3**, 297–315.

KRÖNER, A., LINNEBACHER, P., STERN, R. J., REISCHMANN, T., MANTON, W. & HUSSEIN, I. M. 1991. Evolution of Pan-African island arc assemblages in the southern Red Sea Hills, Sudan, and in southwestern Arabia as exemplified by geochemistry and geochronology. *Precambrian Research* **53**, 99–118.

KRÖNER, A., KRÜGER, J. & RASHWAN, A. A. A. 1994. Age and tectonic setting of granitoid gneisses in the Eastern Desert of Egypt and south-west Sinai. *Geologische Rundschau* **83**, 502–13.

KRÖNER, A., STIPSKA, P., SCHULMANN, K. & JAECKEL, P. 2000. Chronological constraints on the pre-Variscan evolution of the northeastern margin of the Bohemian Massif, Czech Republik. In *Orogenic Processes: Quantification and Modelling in the Variscan Belt* (eds

W. Franke, V. Haak, O. Oncken and D. Tanner), pp. 175–97. Geological Society of London, Special Publication no. 179.

KROGH, T. E. 1973. A low-contamination method for hydrothermal decomposition of zircon and extraction of U and Pb for isotopic age determinations. *Geochimica et Cosmochimica Acta* **37**, 485–94.

LEE, J. K. W., WILLIAMS, I. S. & ELLIS, D. J. 1997. Pb, U and Th diffusion in natural zircon. *Nature* **390**, 159–61.

LIATI, A., GEBAUER, D. & FANNING, C. M. 2004. The age of ophiolitic rocks of the Hellenides (Vourinos, Pindos, Crete): first U–Pb ion microprobe (SHRIMP) zircon ages. *Chemical Geology* **207**, 171–88.

LINNEMANN, U., GEHMLICH, M., TICHOMIROWA, M., BUSCHMANN, B., NASDALA, L., JONAS, P., LÜTZNER, H. & BOMBACH, K. 2000. From Cadomian subduction to Early Palaeozoic rifting: the evolution of Saxo-Thuringia at the margin of Gondwana in the light of single-zircon geochronology and basin development (Central European Variscides, Germany). In *Orogenic Processes: Quantification and Modelling in the Variscan Belt* (eds W. Franke, V. Haak, O. Oncken and D. Tanner), pp. 131–53. Geological Society of London, Special Publication no. 179.

LOOS, S. & REISCHMANN, T. 1999. The evolution of the Menderes Massif in SW Turkey as revealed by zircon dating. *Journal of the Geological Society, London* **156**, 1021–30.

LUDWIG, K. R. 2001. *SQUID 1.02*. Berkeley Geochronological Center, Special Publication no. 2.

LUDWIG, K. R. 2003. *Isoplot/Ex 3.00. A geochronological toolkit for Microsoft Excel.* Berkeley Geochronological Center, Special Publication no. 4.

MARAKIS, G. 1969. Geochronological studies of some granites from Macedonia (in Greek with English summary). *Annales géologiques des pays helleniques* **21**, 121–52.

MATTINSON, J. M., GRAUBARD, C. M., PARKINSON, D. L. & MCLELLAND, W. C. 1996. U–Pb reverse discordance in zircons: the role of fine-scale oscillatory zoning and sub-microscopic transport of Pb. *American Geophysical Union, Geophysical Monograph* **95**, 355–70.

MCNAMARA, A. K., NIOCAILL, C. M., VAN DER PLUIJM, B. A. & VAN DER VOO, R. 2001. West African proximity of the Avalon terrane in the latest Precambrian. *Geological Society of America Bulletin* **113/9**, 1161–70.

MEERT, J. G. 2003. A synopsis of events related to the assembly of eastern Gondwana. *Tectonophysics* **362**, 1–40.

MEZGER, K. & KROGSTAD, E. J. 1997. Interpretation of discordant U–Pb zircon ages: An evaluation. *Journal of Metamorphic Geology* **15**, 127–40.

MICHARD, A., GURRIET, P., SOUDANT, M. & ALBAREDE, F. 1985. Nd isotopes in French Phanerozoic shales: external vs. internal aspects of crustal evolution. *Geochimica et Cosmochimica Acta* **49**, 601–10.

MOST, T., FRISCH, W., DUNKL, I., KADOSA, B., BOEV, B., AVGERINAS, A. & KILIAS, A. 2001. Geochronological and structural investigations of the Northern Pelagonian Crystalline Zone. Constraints from K/Ar and zircon and apatite fission track dating. *Bulletin of the Geological Society of Greece* **XXXIV/1**, 91–5.

MOST, T. 2003. *Geodynamic Evolution of the Eastern Pelagonian Zone in northwestern Greece and the Republic of Macedonia. Implications from U/Pb, Rb/Sr, K/Ar, $^{40}Ar/^{39}Ar$ geochronology and fission track thermochronology.* Published Ph.D. thesis, Universität Tübingen. URN: urn:nbn:de:bsz:21-opus-7057, URL: http://w210.ub.uni-tuebingen.de/dbt/volltexte/2003/705/

MOUNTRAKIS, D. 1982. Étude géologique des terrains métamorphiques de Macédoine occidentle (Grèce). *Bulletin de la Société géologique de France* **24/4**, 697–704.

MOUNTRAKIS, D. 1984. Structural evolution of the Pelagonian Zone in Northwestern Macedonia, Greece. In *The geological evolution of the Eastern Mediterranean* (eds J. E. Dixon and A. H. F. Robertson), pp. 581–90. Geological Society of London, Special Publication no. 17.

MOUNTRAKIS, D. 1986. The Pelagonian Zone in Greece: a polyphase-deformed fragment of the Cimmeran Continent and its role in the geotectonic evolution of the eastern Mediterranean. *Journal of Geology* **94**, 335–47.

MURPHY, J. B. & NANCE, R. D. 2002. Sm-Nd isotopic systematics as tectonic tracers: an example from West Avalonia in the Canadian Appalachians. *Earth-Science Reviews* **59**, 77–100.

MURPHY, J. B., KEPPIE, J. D., DOSTAL, J. & NANCE, R. D. 1999. Neoproterozoic-early Palaeozoic evolution of Avalonia. In *Laurentia–Gondwana Connections before Pangea* (eds V. A. Ramos and J. D. Keppie), pp. 253–66. Geological Society of America, Special Paper no. 336.

NANCE, R. D. & MURPHY, J. B. 1994. Contrasting basement isotopic signatures and the palinspastic restoration of peripheral orogens: Example from the Neoproterozoic Avalonian–Cadomian belt. *Geology* **22**, 617–20.

NANCE, R. D. & MURPHY, J. B. 1996. Basement isotopic signatures and Neoproterozoic paleogeography of Avalonian–Cadomian and related terranes in the circum-North Atlantic. In *Avalonia and related peri-Gondwana terranes of the circum-North Atlantic* (eds R. D. Nance and M. D. Thompson), pp. 333–46. Geological Society of America, Special Paper no. 304.

O'CONNOR, J. T. 1965. A classification of quartz-rich igneous rocks based on feldspar ratios. *U.S. Geological Survey Professional Paper* **525B**, B79–84.

PARRISH, R. 2001. The response of mineral chronometers to metamorphism and deformation in orogenic belts. In *Continental Reactivation and Reworking* (eds J. A. Miller, R. E. Holdsworth, I. S. Buick and M. Hand), pp. 289–301. Geological Society of London, Special Publication no. 184.

PEARCE, J. A., HARRIS, N. B. W. & TINDLE, A. G. 1984. Trace element discrimination diagrams for the tectonic interpretation of granitic rocks. *Journal of Petrology* **25**, 956–83.

PE-PIPER, G. & PIPER, D. J. W. 2002. *The igneous rocks of Greece. The anatomy of an orogen.* Berlin/Stuttgart: Gebrueder Borntraeger, 573 pp.

PE-PIPER, G., DOUTSOS, T. & MIJARA, A. 1993. Petrology and Regional Significance of the Hercynian Granitoid rocks of the Olympiada Area, Northern Thessaly, Greece. *Chemie der Erde* **53**, 21–36.

PE-PIPER, G., DOUTSOS, T. & MPORONKAY, C. 1993. Structure, geochemistry and mineralogy of Hercynian granitoid rocks of the Verdikoussa area, Northern Thessaly, Greece and their regional significance. *Neues Jahrbuch für Mineralogie, Abhandlungen* **165/3**, 267–96.

REISCHMANN, T. 1998. Pre-alpine origin of tectonic units from the metamorphic complex of Naxos, Greece,

identified by single-zircon Pb/Pb dating. *Bulletin of the Geological Society of Greece* **XXXII/3**, 101–11.

REISCHMANN, T., KOSTOPOULOS, D. K., LOOS, S., ANDERS, B., AVGERINAS, A., & SKLAVOUNOS, S. A. 2001. Late Palaeozoic magmatism in the basement rocks southwest of Mt. Olympos, Central Pelagonian Zone, Greece: remnants of a Permo-Carboniferous magmatic arc. *Bulletin of the Geological Society of Greece* **XXXIV/3**, 985–93.

SCHERMER, E. R., LUX, D. R. & BURCHFIEL, B. C. 1990. Temperature-time history of subducted continental crust, Mount Olympos region, Greece. *Tectonics* **9**(5), 1165–95.

ŞENGÖR, A. M. C. & YILMAZ, Y. 1981. Tethyan evolution of Turkey: a plate tectonic approach. *Tectonophysics* **75**, 181–241.

SPRAY, J. G., BÉBIEN, J., REX, D. C. & RODDICK, J. C. 1984. Age constraints on the igneous and metamorphic evolution of the Hellenic-Dinaric ophiolites. In *The geological evolution of the Eastern Mediterranean* (eds J. E. Dixon and A. H. F. Robertson), pp. 619–27. Geological Society of London, Special Publication no. 17.

STACEY, J. S. & KRAMERS, J. D. 1975. Approximation of terrestrial lead isotope evolution by a two-stage model. *Earth and Planetary Science Letters* **26**, 207–21.

STAMPFLI, G. M. & BOREL, G. D. 2002. A plate tectonic model for the Paleozoic and Mesozoic constrained by dynamic plate boundaries and restored synthetic oceanic isochrons. *Earth and Planetary Science Letters* **196**, 17–33.

TAIT, J. A., BACHTADSE, V., FRANKE, W. & SOFFEL, H. C. 1997. Geodynamic evolution of the European Variscan fold belt: palaeomagnetic and geological constraints. *Geologische Rundschau* **86**, 585–98.

TEKLAY, M., KRÖNER, A., MEZGER, K. & OBERHÄNSLI, R. 1998. Geochemistry, Pb–Pb single-zircon ages and Nd–Sr isotope composition of Precambrian rocks from southern and eastern Ethiopia: implications for crustal evolution in East Africa. *Journal of African Earth Sciences* **26**, 207–27.

THOROGOOD, E. J. 1990. Provenance of pre-Devonian sediments of England and Wales: Sm–Nd isotopic evidence. *Journal of the Geological Society, London* **147**, 591–4.

VAVASSIS, I., DE BONO, A., STAMPFLI, G. M., GIORGIS, D., VALLOTON, A. & AMELIN, Y. 2000. U–Pb and Ar–Ar geochronological data from the Pelagonian basement in Evia (Greece): geodynamic implications for the evolution of Palaeotethys. *Schweizerische Mineralogische und Petrographische Mitteilungen* **80**, 21–43.

VAVRA, G. 1990. On the kinematics of zircon growth and its petrogenetic significance: a cathodoluminescence study. *Contributions to Mineralogy and Petrology* **106**, 90–9.

VON RAUMER, J. F., STAMPFLI, G. M. & BUSSY, F. 2003. Gondwana-derived microcontinents – the constituents of the Variscan and Alpine collisional orogens. *Tectonophysics* **365**, 7–22.

WENDT, J. I. & TODT, W. 1991. A vapour digestion method for dating single zircons by direct measurement of U and Pb without chemical separation. *Terra Abstracts* **3**, 507–8.

WHITE, W. M. & PATCHETT, J. 1984. Hf–Nd–Sr isotopes and incompatible element abundances in island arcs: implications for magma origins and crust-mantle evolution. *Earth and Planetary Science Letters* **67**, 167–85.

WILLIAMS, I. S. 1992. Some observations on the use of zircon U–Pb geochronology in the study of granitic rocks. *Transactions of the Royal Society of Edinburgh: Earth Sciences* **83**, 447–58.

YARWOOD, G. A. & AFTALION, M. 1976. Field relations and U–Pb geochronology of a granite from the Pelagonian Zone of the Hellenides (High Pieria, Greece). *Bulletin de la Société Géologique de France* **18/2**, 259–64.